

UNCLASSIFIED

AD 289 213

*Reproduced
by the*

**ARMED SERVICES TECHNICAL INFORMATION AGENCY
ARLINGTON HALL STATION
ARLINGTON 12, VIRGINIA**



UNCLASSIFIED

DISCLAIMER NOTICE

THIS DOCUMENT IS BEST QUALITY PRACTICABLE. THE COPY FURNISHED TO DTIC CONTAINED A SIGNIFICANT NUMBER OF PAGES WHICH DO NOT REPRODUCE LEGIBLY.

NOTICE: When government or other drawings, specifications or other data are used for any purpose other than in connection with a definitely related government procurement operation, the U. S. Government thereby incurs no responsibility, nor any obligation whatsoever; and the fact that the Government may have formulated, furnished, or in any way supplied the said drawings, specifications, or other data is not to be regarded by implication or otherwise as in any manner licensing the holder or any other person or corporation, or conveying any rights or permission to manufacture, use or sell any patented invention that may in any way be related thereto.

63-1-4

289213

CATALOGED BY ASTIA
AS AD NO. _____

ELECTROCHEMISTRY RESEARCH LABORATORY

DEPARTMENT OF CHEMISTRY
WESTERN RESERVE UNIVERSITY
CLEVELAND, OHIO

TECHNICAL REPORT NO. 15

THE ELECTROCHEMISTRY OF NICKEL
II. Anodic Polarization of Nickel

by

M. L. Kronenberg, J. C. Banter, E. Yeager, and F. Hovcrka

October 15, 1962

OFFICE OF NAVAL RESEARCH

Contract Nonr 2391(00)

Project NR 359-277

OFFICE OF NAVAL RESEARCH

Contract Nonr 2391(00)

Project NR 359-277

TECHNICAL REPORT 15

THE ELECTROCHEMISTRY OF NICKEL

II. Anodic Polarization of Nickel

by

M. L. Kronenberg, J. C. Banter, E. Yeager, and F. Hovorka

Department of Chemistry
Western Reserve University
Cleveland, Ohio

October 15, 1962

Reproduction in whole or part is permitted for any purpose of
the United States Government.

THE ELECTROCHEMISTRY OF NICKEL
II. Anodic Polarization of Nickel

M. L. Kronenberg,¹ J. C. Banter,² E. Yeager, and F. Hovorka
Department of Chemistry, Western Reserve University
Cleveland, Ohio

ABSTRACT

The anodic dissolution of nickel has been studied in acidified chloride, sulfate, and perchlorate solutions under a variety of non-passivating conditions. The Tafel slopes at 45°C are approximately 0.085, 0.115, and 0.12, respectively. The lower value of the Tafel slope in chloride solutions is attributed to specific adsorption. The potential of the nickel anode is independent of Ni^{+2} concentration under conditions for which the back reaction is negligible and no pH dependence has been found for pH of 1 to 2.5. The temperature dependence of the polarization yields an approximate value of 15 kcal/mole for the heat of activation in the chloride solution.

¹ Now at the Research Laboratory of Union Carbide Consumer Products Company, Division of Union Carbide Corporation, Parma, Ohio.

² Now at the Oak Ridge National Laboratory, Oak Ridge, Tenn.

Technical Report 15

THE ELECTROCHEMISTRY OF NICKEL

II. Anodic Polarization of Nickel

by

M. L. Kronenberg, J. C. Banter, E. Yeager, and F. Hovorka

The electrodeposition of nickel has been the subject of many experimental investigations. With the exception of studies of anodic passivation, however, relatively little fundamental research effort has been directed toward an understanding of the anodic dissolution reaction. Where data are available, much of it is not conducive to fundamental analysis and interpretation. Of particular interest is the work cited in references (1-9).

The purpose of the present work has been to obtain information concerning the mechanism of the anodic dissolution of nickel. The anodic polarization has been measured as a function of current density, temperature, pH, concentration of nickel ion, nature and concentration of supporting electrolyte, and the source and crystallographic orientation of the nickel anode.

Apparatus

The indirect method has been used for the polarization measurements. This method was favored because it avoids some of the difficulties associated with the use of a Luggin capillary and because of the availability of equipment at Western Reserve University.

A block diagram of the electronic interrupter and its associated equipment is shown in Figure 1. The current from the polarizing source is interrupted when repetitive rectangular negative pulses from the pulse generator are applied to the grids of parallel-connected triodes (6SN7) or beam power pentodes (6L6), driving them to cut off (10). For most of the results reported here the current was off for 50 microsec and on for 1300 microsec. These times, which represent a 96 per cent duty cycle, were sufficient to permit buildup of the potential to a steady-state value prior to interruption.

By means of the differential amplifier, the anode-reference, cathode-anode, and cathode-reference potential could be viewed on the oscilloscope (Tektronic type 512). The potential difference associated with any portion of the buildup or decay curve could be measured to ± 1 mv ± 0.1 per cent (whichever is larger) by adjusting potentiometers A and B (Figure 1) so as to bring that portion of the trace on the oscilloscope screen to the zero deflection position. Switching transients were such that the potential could be measured

within 1 to 3 microsec following interruption of the current. A complete circuit diagram is given elsewhere (10). A Leeds & Northrup K-2 potentiometer was used to measure the potentials between the reference electrodes involved in this work.

The glass polarization cell is similar to that described in the first paper (11) in this series. Provisions are made for various reference and pre-electrolysis electrodes in addition to the anode and cathode involved in the polarization measurements. The cell provides for a controlled relatively high speed flow of the solution past the anode at rates up to 60 cm/sec in the bulk of the solution adjacent to the anode. The voltage from an electric tachometer was used as a relative measure of the solution velocity. The tachometer was calibrated in terms of flow rates under experimental conditions by means of a pitot tube as described earlier (11). The cell was mounted in a thermostatic bath which controlled the temperature to $\pm 0.05^{\circ}\text{C}$ in the range 25 to 45°C .

The hydrogen gas used for saturating the solution was passed through a purification train consisting of the following components:

1. De-Oxo unit for catalytic oxygen removal (Baker Co. Inc., Newark, N. J.)
2. magnesium perchlorate for drying
3. Hopcalite for oxidation of trace CO (Mine Safety Appliance Co., Pittsburgh, Pa.)

4. soda lime for removal of CO_2 and H_2O
5. three liquid nitrogen cooled traps for the adsorption of impurities with the first filled with silica gel, the second with active carbon, and the third with glass wool

Experimental Procedure

Several anode designs and sources of nickel were compared in preliminary experiments. The anodes were designed to provide a reasonably uniform current density over the surface of the electrode. The first electrodes used were 14-gauge (B. and S.) nickel wire of 99% purity and Johnson-Matthey nickel rod which was machined down to 3mm in diameter. Both types were sealed in 8-mm O.D. soft glass and were rounded at the end to essentially the same radius of curvature as the cylindrical portion.

Efficiency measurements were obtained using an anode consisting of Johnson-Matthey nickel rod cut down to 3 mm in diameter. One end of the rod was drilled and tapped to fit the threaded end of the 14-gauge nickel wire which was sealed in soft glass. This permitted the direct weighing of the anode used in efficiency measurements. The design is shown in Figure 2a. For current densities above 0.3 ma/cm^2 efficiencies could be measured with a precision of ± 2 per cent.

The electrode design adopted for single crystal electrodes is shown in Figure 2b. This design permitted polarization measurements at a particular face of a single

crystal without introducing any plastics or organic sealers into the electrolyte. One face of the cylindrical nickel electrode was drilled and tapped and a threaded contact was made with nickel wire. The other face was kept even with the glass tubing so that only the desired face was exposed to the electrolyte. Hydrogen gas from the purification train flowed between the metal and glass to prevent the solution from flowing up the tube. The hole in the top of the glass through which the nickel wire passes was sealed with melted polyethylene. The ground glass joint facilitated removal and preparation of the anode.

The various nickel anodes all gave substantially the same results for the polarization when differences in the ratio of true to apparent area are taken into account. In the present work, the differences in the differential capacity between various electrodes at a given potential have been used as a criterion of relative changes in electrode area. The differential capacity c has been calculated from the initial rate of decay of the polarization following interruption of the polarizing current by means of the equation

$$c = i / \left(\frac{dE}{dt} \right)_0 \quad (1)$$

where i is the current and $(dE/dt)_0$ is the initial rate of decay of the potential.

Individual measurements of differential capacity were limited to an accuracy of ± 10 per cent because of of diffi-

difficulties associated with the determination of the slope from the oscilloscope trace. A small amount of 60-cycle pick-up, amounting to 0.7 mv, also was evident on the oscilloscope and limited the accuracy of the capacitance measurements.

The source of the nickel made a difference in the ease of obtaining reproducible polarization data. Nickel electrodeposited from a bath containing carefully purified nickel chloride and nickel sulfate exhibited the most rapid area changes upon dissolution. This made it difficult to obtain reproducible polarization data. The measurements with such electrodes had to be made quickly and even then were restricted to low current densities. The 14-gauge nickel wire and Johnson-Matthey nickel dissolved anodically with relatively minor area changes during short polarization runs. The Johnson-Matthey electrodes gave the most reproducible results. Unless otherwise indicated, Johnson-Matthey nickel electrodes were used for all the data presented in this paper.

The cathode used for the pre-electrolysis and polarization measurements consisted of a square piece of platinum foil, 2.5 cm on an edge and 0.01 cm thick, attached to a platinum wire sealed in soft glass tubing. The pre-electrolysis anode also was platinum and of similar construction. Platinum was used for the pre-electrolysis anode to eliminate the possible introduction of impurities

that might have resulted from a dissolving nickel pre-electrolysis anode.

Two types of reference electrodes were used for the polarization runs. A Pt-Pt electrode was used as a working reference electrode within the cell. It was prepared by sealing platinum wire in soft glass and platinizing it in a 1 per cent solution of platinic chloride (without any additives) at 100 ma/cm^2 for approximately 2 hr. with periodic reversal of the current every 5 min. (12). After platinizing, the electrodes were stored in slightly acidified conductivity water which was saturated with hydrogen.

A saturated calomel reference was used with chloride and perchlorate solutions and a mercury-mercurous sulfate, saturated potassium sulfate reference was used with the sulfate solutions to check the working reference electrode before and after each polarization run. To avoid the introduction of any contaminants into the electrolyte from the external reference electrode, a solution bridge filled with the same solution as in the cell was used between the cell and an intermediate vessel (test tube) containing the same solution as in the cell. The external reference electrode was connected to this intermediate vessel by a second solution bridge. The reference electrode and intermediate vessel were immersed in the same water bath as the cell.

The polarization measurements, with the exception of

those in the sodium perchlorate solutions, were obtained in solutions prepared from Fisher certified reagent-grade salts which were further purified by double recrystallization from conductivity water. The sodium perchlorate solutions were prepared from reagent grade chemicals and conductivity water.

The anode was prepared for polarization measurements by polishing with progressively finer grades of emery paper down to 000 grade. It was then immersed in ethyl alcohol and rinsed in distilled water. In most instances the anode was then electropolished for 20 min at 150 ma/cm^2 in an electropolishing solution containing 15 per cent H_2SO_4 , 63 per cent H_3PO_4 , and 22 per cent H_2O (13). The nickel anode was rinsed copiously in distilled and conductivity water before being placed in the polarization cell. Unless otherwise indicated, all polarization curves presented in this paper were obtained with electropolished electrodes.

The platinum pre-electrolysis anode was placed in the anode compartment during pre-electrolysis and removed entirely from the electrolyte when pre-electrolysis was completed. During pre-electrolysis the platinum anode was in the main flow stream and stirring was maintained throughout the pre-electrolysis period. Pre-electrolysis was carried out at 20 microamp/cm^2 . This low current density did not produce appreciable pH changes during the pre-electrolysis period and was below the limiting current density for the oxidation of molecular hydrogen. During the pre-

electrolysis the platinum anode was at a potential near the upper limit (numerically) reached during the anodic polarization run. The potential of the pre-electrolysis anode never approached that for the oxygen evolution reaction. The effectiveness of pre-electrolysis under these conditions is far from certain. This procedure, however, did lead to reproducible results.

In preparation for polarization measurements the cell was rinsed several times first with distilled and conductivity water and finally with the solution to be investigated. The cell then was filled with solution and the electrodes were introduced into the solution after appropriate rinsings. Hydrogen gas was then bubbled into the solution, the stirrer was turned on, and the system was allowed to come to equilibrium. The pH was adjusted by addition of the appropriate acid and was determined by measuring the potential between the Pt-Pt reference electrode within the cell and the external reference electrodes. The accuracy of the pH measurements is open to question because of the unknown liquid-junction potential. Pre-electrolysis was then begun. The solutions were pre-electrolyzed in the cell for 40 hr to remove trace impurities or at least to reduce their concentration to a reproducible minimum. A polarization run was then made and the pre-electrolysis was resumed for 6 to 8 hr. A polarization run was made again after this second pre-electrolysis period and if both runs agreed within several millivolts,

pre-electrolysis was regarded as complete.

After pre-electrolysis the working nickel electrode was anodically dissolved at 0.5 ma/cm^2 for 5 min prior to the beginning of polarization measurements. Polarization measurements were taken by adjusting the current and quickly measuring the anode potential relative to the internal working reference electrode after the potential had reached a reasonably constant value. This usually required less than 30 sec. Between polarization measurements while the current through the electronic equipment was being adjusted to a new value, the electrodes were disconnected from the circuit to minimize anode area changes.

Efficiency measurements were made by direct weighing of the anode using the detachable anode assembly described earlier. The coulombs passed were determined with a coulometer or from the time and IR drop across a precision resistor which was connected in series with the commutator circuit. Efficiency measurements were made at constant potential under conditions analogous to a polarization run. The time for each efficiency run was at least one hour.

Experimental Results

Anode efficiencies for nickel dissolution in chloride solutions of pH 2.0 to 3.0 were within a few per cent of 100 per cent in the potential range which corresponded to current densities of 0.3 to 15 ma/cm^2 . Efficiencies in perchlorate and sulfate solutions of pH 2.0 to 3.0 were

difficult to determine because of a tendency toward passivation upon prolonged anodic dissolution even at moderate current densities. In several instances where the anode did not passivate, the efficiencies were less than 50 per cent at potentials corresponding to current densities less than approximately 0.6 ma/cm^2 . This indicates that hydrogen dissolution predominates under these conditions. For pH of 0.9 to 1.0, nickel dissolution efficiencies in perchlorate and sulfate solutions were virtually 100 per cent over the range 0.3 to 5 ma/cm^2 in instances where the anode did not passivate.

The differential capacitance has been found to be strongly dependent on the method of preparation of the nickel anode. Nickel anodes prepared by electropolishing normally had a differential capacitance of $20 \mu\text{F/cm}^2$ of apparent area in the 0.5 M NiCl solution. This value was substantially independent of potential over the range 0 to $+0.15 \text{ v}$ relative to the standard hydrogen electrode. Nickel electrodes only finished by hand polishing with successively finer grades of emery paper down to 000 grade had differential capacitances of approximately $35 \mu\text{F/cm}^2$ of apparent area over the same range of potentials. The differential capacitance depended also on the source of the nickel. For example, electropolished nickel wire and also electrodeposited nickel with no surface treatment after deposition had higher values than electropolished pure Johnson-Matthey nickel.

The differential capacitance usually increased slowly

during the anodic dissolution. This area change normally was less than 10 per cent during the course of a single polarization run because the electrodes were disconnected between measurements to limit progressive area changes during dissolution.

The anode potential-current density curves for several electrolytes are compared in Figure 3. The potentials are given relative to the standard hydrogen electrode and the current densities are based on apparent areas. These curves show that a Tafel relationship exists for nickel in the various electrolytes and that the anode potential at a given current density is dependent on the type of electrolyte. The polarization in the chloride solution is substantially lower than in the perchlorate or sulfate solutions. The current efficiency for the metal dissolution was close to 100% for all three curves in Figure 3. It was necessary to reduce the pH to 1.0 for the perchlorate and sulfate solutions, however, to accomplish this.

In the linear Tafel region, the back reaction should be negligible and the polarization should not depend on Ni^{+2} concentration provided double properties remain constant. This appears to be true from the data in Figure 4. Identical polarization data have been obtained with and without Ni^{+2} present up to 0.1 M Ni^{+2} provided an excess of a supporting electrolyte was present. Most of the subsequent measurements have been made without Ni^{+2} present.

This avoids the necessity of purifying nickel salts, which are ordinarily difficult to purify because of problems associated with crystallization.

The differences in the anodic potentials at a given current density in Figure 3 are not due principally to the presence or absence of Ni^{+2} . Differences in the double layer and in particular anion adsorption are probably the main factors responsible for the differences evident in this figure. Variations in liquid-junction potential also are involved but probably are a minor factor.

The absence of Ni^{+2} in the solution does cause some awkwardness regarding absolute polarization values and the calculation of exchange current densities because of undefined reversible conditions. The apparent exchange current density depends on the Ni^{+2} concentration, which influences the reversible potential. In the present work the equivalent of an exchange current density has been obtained even in the absence of Ni^{+2} by extrapolatory the linear Tafel curves to a potential corresponding to the standard electrode potential. This value obtained by extrapolation will be referred to as the standard exchange current density in this paper. It represents the exchange current density which would be found experimentally for a solution containing Ni^{+2} at unity activity if the transfer coefficients and double layer properties remained unchanged over a range of potentials extending from the linear Tafel region to the reversible value.

The dependence of the potential on concentration at a given current density is very slight in sodium perchlorate

solutions in the absence of Ni^{+2} over the concentration range 0.25 M to 1.0 M on the basis of the data in Figure 5. The linear range for nickel dissolution at pH 2.5 in the perchlorate solutions is quite limited because of the competing hydrogen oxidation reaction at low current densities and passivation at higher current densities. Unfortunately efficiency data were not available for the perchlorate system. The section of the curve below the inflection point, however, is associated primarily with H_2 anodic dissolution. An attempt has been made to construct the individual polarization curves for nickel and hydrogen dissolution in Figure 5. The assumption has been made that the Tafel slope for the nickel dissolution curve does not change over the entire range of the plot. The procedure used in obtaining the component polarization curves in Figure 5 involved first making an estimate of the limiting current density for H_2 oxidation. This value was then subtracted from the total current density for the upper portion of the overall polarization curve and the component polarization curve for nickel dissolution constructed. The extension of this curve for nickel to current densities below the inflection point in the overall polarization curve permitted the evaluation of the curve for H_2 oxidation. If the limiting current density indicated by this curve differed significantly from the original estimate, the complete process was repeated with a new estimate for the limiting current density for H_2 oxidation.

The procedure just described is not a very satisfactory substitute for current efficiency data in evaluating the H₂ oxidation curve and the authors hope to undertake a study in which such data are obtained in the future. To the best knowledge of the authors, the polarization curve for H₂ oxidation represents the first time that such data have been available in acid media even on a provisional basis. The slope is 0.13 over the limited linear range represented in Figure 5. This slope should not be interpreted as the ordinary Tafel slope because of the proximity of the limiting current density to the short range over which the apparent slope of 0.13 v per decade is exhibited.

A polarization curve similar to that in Figure 5 has been obtained for a 0.5 M NiSO₄ at pH 2.5 and 45°C. The apparent Tafel slope for H₂ oxidation in the NiSO₄ electrolyte is 0.11 v per decade.

The polarization curves in Figure 6 indicate the effect of a 10 and 100 fold change in KCl concentration in the absence of Ni⁺². The efficiency for nickel dissolution has been found to be substantially 100% for all points in this figure. The decrease in polarization with increasing KCl concentration appears reasonable in terms of the concentrating dependence which various workers (14-16) have estimated for the potential drop across the diffuse ionic layer. A quantitative comparison, however, is seriously complicated by specific adsorption, close proximity to the zero point of charge, and the liquid-junction potentials

involved in the comparison of the internal hydrogen reference electrode with the external saturated calomel reference electrode (necessary for the calculation of the potentials of the polarized anode relative to the standard hydrogen electrode).

The increase in Tafel slope in 0.01 M KCl at current densities greater than 2 ma/cm² was observed each of several times the experiment was repeated. The explanation is open to speculation. One possibility is that the nickel concentration in the solution in the immediate vicinity of the electrode surface became appreciably compared to the concentration of KCl in the dilute KCl solution and a change in double layer properties occurred. A significant portion of the nickel would probably be involved in a chloride complex.

The dependence of anode potential on temperature in KCl, NaClO₄, and NiCl₂ solutions is shown in Figures 7-9. In all cases, the anode potential decreases 2.7 ± 0.3 mv per °C increase in temperature for a given apparent current density.

The results shown in Figure 10 indicate that no appreciable charge occurs in the anodic polarization over the pH range 2 to 3 in 1.0 M KCl at 45°C under conditions where the efficiency for nickel dissolution is substantially 100%. The anodic polarization also has been found to be independent of pH in the range 1. to 2.5 in 0.5 M NiSO₄ over the current density range 0.8 to 4.0 ma/cm² where the efficiency for the nickel dissolution process is virtually 100%.

Hollnagel and Landsberg (8) report finding a pH dependence for the anodic dissolution of nickel in both chloride and sulfate solutions in measurements of non-steady state polarization with a galvanostatic method involving rectangular current pulses. Their findings, however, may be somewhat misleading since the concentration of the supporting electrolyte was not large compared to the concentration of the acid added in adjusting the hydrogen ion concentration.

Polarization measurements have also been made with electropolished single crystal nickel anodes. The results are essentially the same as obtained with polycrystalline nickel. Figure 11 compares the polarization obtained on a surface parallel to the 110 plane with that for a polycrystalline anode of Johnson-Matthey nickel. The orientation of a particular crystallographic plane parallel to the electrode surface does not ensure that other crystallographic planes are not exposed to the electrolyte; i.e., the micro-orientation of the surface need not and in most cases probably does not correspond to the macro orientation.

The Tafel slopes and standard exchange current densities based on apparent areas are listed in Table 1. All of the data in this table were obtained under conditions for which the efficiency of the nickel dissolution process was substantially 100%. In most instances the Tafel linearity has been observed over a current density range of at least 1-1/2 decades and in many instances 2 decades. The standard

exchange current densities have been determined by extrapolating the linear Tafel plots to the standard electrode potential of nickel. The latter have been evaluated at the various temperatures by the same procedure used in the first paper in this series (11). The values calculated by this means are probably accurate to ± 10 mv. The accuracy of the values for the standard exchange current densities, however, is limited more by the accuracy of the Tafel slope and the surface roughness than the accuracy of the values for the standard electrode potential.

Discussion of Experimental Results

From Table 1 it is evident that the Tafel slope at 45°C is 0.11 to 0.12 in both sulfate and perchlorate solutions. The Tafel linearity and the value of the Tafel slope provide evidence favoring a charge transfer step as rate determining. For a Tafel slope of 0.12, the corresponding value of αz is 0.52 where α is the transfer coefficient and z the charge of the species transferred over the potential energy barrier associated with the rate-determining step. The lower Tafel slope of 0.08 to 0.09 found for the chloride solutions probably reflects the specific adsorption of chloride ions on the electrode surface and the associated changes in the overall double layer structure (see for example ref. 16). The adsorption of Cl^- on the anode surface is anticipated to favor the transfer of nickel from the metallic state to a position

in the Helmholtz plane as an adsorbed ionic species.

In the earlier study of nickel electrodeposition the Tafel slope in a 0.5 M nickel sulfate solution was found to be 0.091 at 45°C. A comparison of the Tafel slopes for the anodic and cathodic processes would prove interesting if it were not that the point of zero charge (pzc) is very likely interposed between the two sets of polarization measurements. For the sulfate and perchlorate solutions the pzc is estimated to be -0.1 to -0.2 v relative to the standard hydrogen electrode on the basis that the difference in the pzc for nickel and mercury in a given electrolyte is the same as the difference in the work function (17,18). Thus it is not surprising that the anodic and cathodic Tafel slopes are not complimentary (19) for any reasonable (integer) value of the stoichiometric number.

The heat of activation ΔH^\ddagger at the reversible potential may be calculated by the equation

$$\frac{d \ln i_0}{d (1/T)} = \frac{\Delta H^\ddagger}{R} \quad (2)$$

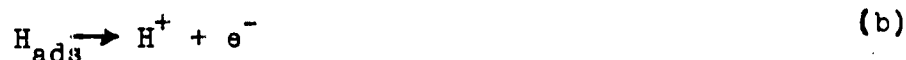
where T is the absolute temperature, i_0 the exchange current density, and R the gas constant. An attempt has been made to use this equation with the data for the NiCl_2 solution in Figure 9. To determine the temperature dependence of $\ln i_0$, it is necessary to extrapolate the linear Tafel plots over five decades to the reversible potentials. Even a slight error in the relative values for the Tafel slopes produces a large error in the derivative. If the Tafel plots

for 25°C and 45°C in Figure 9 are extrapolated independently to the reverse potential, the resulting value for ΔH^\ddagger is 8 kcal/mole. The reversible potentials at 25°C and 45°C have been calculated by the same procedure as used in the earlier paper (11) with the temperature dependence of the ionic activity coefficient for nickel assumed to be negligible.

An alternate procedure is to assume that the transfer coefficient does not vary significantly with temperature. The Tafel slopes for 25°C and 45°C then should be in the same ratio as the absolute temperatures. If the extrapolation of the curves for 25°C and 45°C in Figure 9 is done with the Tafel slope at 45°C taken as $\frac{20}{298} \times 100\%$ or 6.7% greater than that at 25°C, the resulting value for ΔH^\ddagger is 15 kcal/mole. This higher value for ΔH^\ddagger is believed to be more reliable than the lower value despite the assumption concerning the constancy of the transfer coefficient. An additional assumption is that the ratio of true to apparent surface area is independent of temperature. The value found for the heat of activation for the reverse nickel electrodeposition process in the earlier paper (11) was 21 kcal/mole.

An attempt at explaining the H₂ oxidation curve in Figure 5 is premature at this time in view of the very limited current density range of the curve and the assumptions involved in the construction of the curve from the overall anodic polarization curve. Furthermore, the limiting

current density, which appears to be diffusion controlled, interferes with any simple direct interpretation of the apparent Tafel slope. These complications in the direct interpretation of the apparent Tafel slope are well illustrated by the consideration of the following mechanism for H₂ oxidation under circumstances of high and low surface coverage with adsorbed hydrogen.



The H₂ oxidation curve in Figure 5 does not appear compatible with reaction a as the rate determining step at current densities well below the limiting current density because the polarization is too large. Of course, as the diffusion-controlled limiting current density is approached, reaction a will eventually become quite irreversible since the concentration of H₂ will be depressed to zero.

When reaction b is rate determining and the kinetic limiting current density associated with reaction a is very high compared to the diffusion limiting current density, the current density for H₂ oxidation is related to the hydrogen polarization η by the equation

$$i = i_0 \left[\frac{(i_L - i)^{1/2}}{i_L^{1/2}} \cdot \frac{1 + \kappa (P_{\text{H}_2})^{1/2}}{1 + \kappa (P_{\text{H}_2})^{1/2} \left(\frac{i_L - i}{i_L}\right)^{1/2}} \right] \exp \frac{\alpha f \eta}{RT} \quad (3)$$

where i_L is the diffusion limiting current density, i_0 is

the apparent exchange current density, P_{H_2} is the hydrogen saturation pressure (1 atm), α is the transfer coefficient, κ is a constant corresponding to the ratio of the rate constants for the forward and reverse directions for reaction a, and the other symbols have their usual meanings. This equation is derived by setting the forward and reverse rates for reaction a equal to each other, solving for the fraction θ of the surface sites occupied by H_{ads} , and then using this value for θ in the usual kinetic equation for reaction b with the reverse reaction assumed negligible and the concentration of the dissolved H_2 adjacent to the electrode assumed proportional to $(i_L - i)$. The potential drop across the ionic diffuse layer has been assumed not to vary significantly with η .

When $\theta \ll 1$, then $\kappa P_{H_2} \ll 1$, and eq. 3 becomes

$$\eta = -\frac{RT}{\alpha f} \ln i_0 + \frac{RT}{\alpha f} \ln \left[i \left(\frac{i_L - i}{i_L} \right)^{1/2} \right] \quad (4)$$

For $\theta \cong 1$ over the range of potentials of interest, $\kappa P_{H_2} \gg 1$ and

$$\eta = -\frac{RT}{\alpha f} \ln i_0 + \frac{RT}{\alpha f} \ln i \quad (5)$$

Thus for this mechanism if θ is assumed small, a plot of η vs. $\ln \left\{ i \left[\frac{(i_L - i)}{i_L} \right]^{1/2} \right\}$ should be linear rather than just the ordinary Tafel plot of η vs. $\ln i$. If θ is assumed equal to approximately unity, the conventional Tafel linearity may

be anticipated. Unfortunately the range over which the polarization for H_2 oxidation can be constructed in Figure 5 as well as the reliability of the curve are too limited to test which type of dependence is experimentally observed. If the polarization curve for H_2 oxidation is used to establish the slope as given in eq. (4), then $(2.3 RT/\alpha f) = 0.09$ and for $\theta \ll 1$, $\alpha = 0.7$. If $\theta \cong 1$, however, $(2.3 RT/\alpha f) = 0.13$ from the H_2 curve in Figure 5, and $\alpha \cong 0.5$.

The situation is similarly ambiguous for the alternate mechanism involving the reaction $H_2 \longrightarrow H_{ads} + H^+ + e^-$ followed by reaction b.

Summary

In summary, the following has been demonstrated in the present work:

1. The polarization curves for nickel dissolution have been shown to follow Tafel linearity over at least 1.5 decades and in some instances 2 decades in acidified chloride, sulfate, and perchlorate solutions with the apparent Tafel slopes in sulfate and perchlorate solutions equal to 0.12 ± 0.01 and in chloride solutions equal to 0.085 ± 0.005 at $45^\circ C$.
2. With proper buffering of the ionic double layer with a supporting electrolyte, the polarization has been shown to be independent of pH over a limited range.
3. The potential is independent of Ni^{+2} concentration over the range of potentials where the back reaction is negligible.
4. The energy of activation for the anodic dissolution process is approximately 15 kcal/mole if the transfer coefficient and the surface roughness are assumed to be independent of temperature for a dissolving nickel anode.
5. Anodic polarization measurements on single crystal

(110 orientation) and polycrystalline nickel have not been found to differ significantly.

6. Hydrogen dissolution can occur simultaneously with nickel dissolution with the apparent Tafel slope of the polarization curve for the H_2 oxidation equal to 0.13.

References

1. N. Murphy and B. Oza, Bull. Virginia Polytech. Inst. 51 No.7 (1958).
2. F. Salt, Discussions Faraday Soc. 1, 169 (1947).
3. D. Turner, J. Electrochem. Soc. 98, 434 (1951).
4. R. Piontelli and G. Serravalle, Z. Elektrochem. 62, 759 (1958).
5. J. Higgins, J. Electrochem. Soc. 106, 999 (1959).
6. E. Raub and A. Besam, Metalloberfläche 13, 308, (1959).
7. W. Wesley, Trans. Inst. Metal Finishing 33, 452 (1956).
8. M. Hollnagel and R. Landsberg, Z. physik. Chem.(Leipzig) 212, 94 (1959).
9. C. Chang, V. Krautsov, and Y. Durdin. Zhur. Fiz. Khim. 34, 2041 (1960). V. Krautsov and C. Chang, *ibid.* 34, 2205 (1960).
10. E. Yeager, T. Oey, and F. Hovorka, Tech. Report 6, ONR Contract Nonr 47002, Western Reserve University, June, 1952.
11. J. Yeager, J. Cels, E. Yeager, and F. Hovorka, J. Electrochem. Soc. 106, 328 (1959).
12. J. Bockris, private communication.
13. C. Faust and H. Pray, Proc. Am. Electroplaters Soc. 1941, 104.
14. A. Frumkin, et al, Kinetics of Electrode Processes, Moscow University Publishers, Moscow, 1952.
15. M. Breiter, M. Kleinerman, and P. Delahay, J. Am. Chem. Soc. 80, 5111 (1958).
16. R. Parsons in P. Delahay (ed.) Advances in Electrochemistry and Electrochemical Engineering, Vol. 1, Chapter 1, Interscience Publishers, New York, 1961.
17. A. Frumkin, Colloid. Symp. Annual 7, 89 (1930).
18. See also R. Parsons in J. Bockris (ed.), Modern Aspects of Electrochemistry, Vol. 1, Chapter 3, Academic Press, New York, 1954, p. 170.
19. See for example J. Bockris, *loc. cit.* pp. 187, 188.

Table 1. Tafel slopes and standard exchange current densities for anodic oxidation of nickel.

electrolyte	pH	temperature	Tafel slope	current density range for Tafel slope	standard ⁺ exchange current density
1.0 M KCl	2.6	25°C	0.084	0.25-13.0 ma/cm ²	1.4x10 ⁻⁷ ma/cm ²
1.0 M KCl	2.6	35	0.082	0.25-11.0	1.8x10 ⁻⁷
1.0 M KCl	2.6	45	0.080	0.22-12.0	2.8x10 ⁻⁷
0.1 M KCl	2.5	45	0.084	0.05-4.0	1.8x10 ⁻⁷
0.01 M KCl	2.5	45	0.084	0.05-1.2	1.0x10 ⁻⁷
1.0 M NaClO ₄	0.9	27	0.125	0.5-9.0	2.3x10 ⁻⁷
1.0 M NaClO ₄	0.9	44	0.13	0.6-9.0	5.0x10 ⁻⁷
0.25 M NaClO ₄	2.5	45	0.11	0.55-3.0	3.0x10 ⁻⁷
1.0 M NaClO ₄	2.5	45	0.11	0.55-3.0	3.0x10 ⁻⁷
0.5 M NiCl ₂	2.5	25	0.090	0.08-7.0	1.35x10 ⁻⁷
0.5 M NiCl ₂	2.5	35	0.085	0.07-7.0	1.27x10 ⁻⁷
0.5 M NiCl ₂	2.5	45	0.090	0.08-9.0	3.1x10 ⁻⁷
0.5 M NiSO ₄	1.0	45	0.115	0.07-4.0	3.6x10 ⁻⁷

⁺ See text for definition; based on apparent area.

FIGURE CAPTIONS

- Figure 1. Block diagram of electronic interrupter and associated equipment.
- Figure 2. Special electrode designs.
- Figure 3. Potential dependence on nature of electrolyte.
- Figure 4. Dependence on addition of NiCl_2 to 1.0 M KCl .
- Figure 5. Potential dependence on concentration of NaClO_4 .
- Figure 6. Potential dependence on concentration of KCl .
- Figure 7. Potential dependence on temperature in 1.0 M KCl .
- Figure 8. Potential dependence on temperature in 1.0 M NaClO_4 .
- Figure 9. Potential dependence on temperature in 0.5 M NiCl_2 .
- Figure 10. Potential dependence on pH in 1.0 M KCl .
- Figure 11. Comparison of polycrystalline and single crystal nickel in 1.0 M KCl .

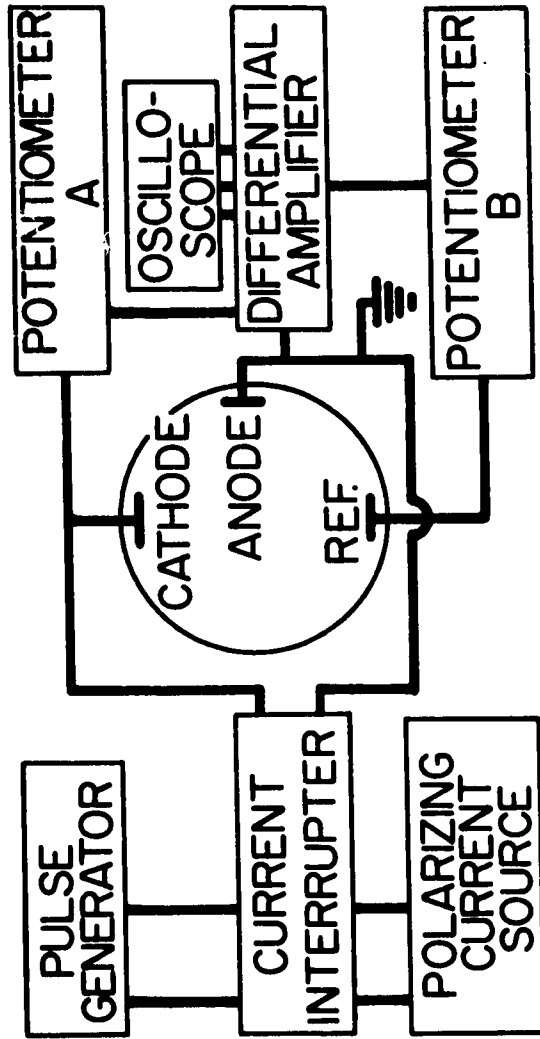


Figure 1. Block diagram of electronic interrupter and associated equipment.

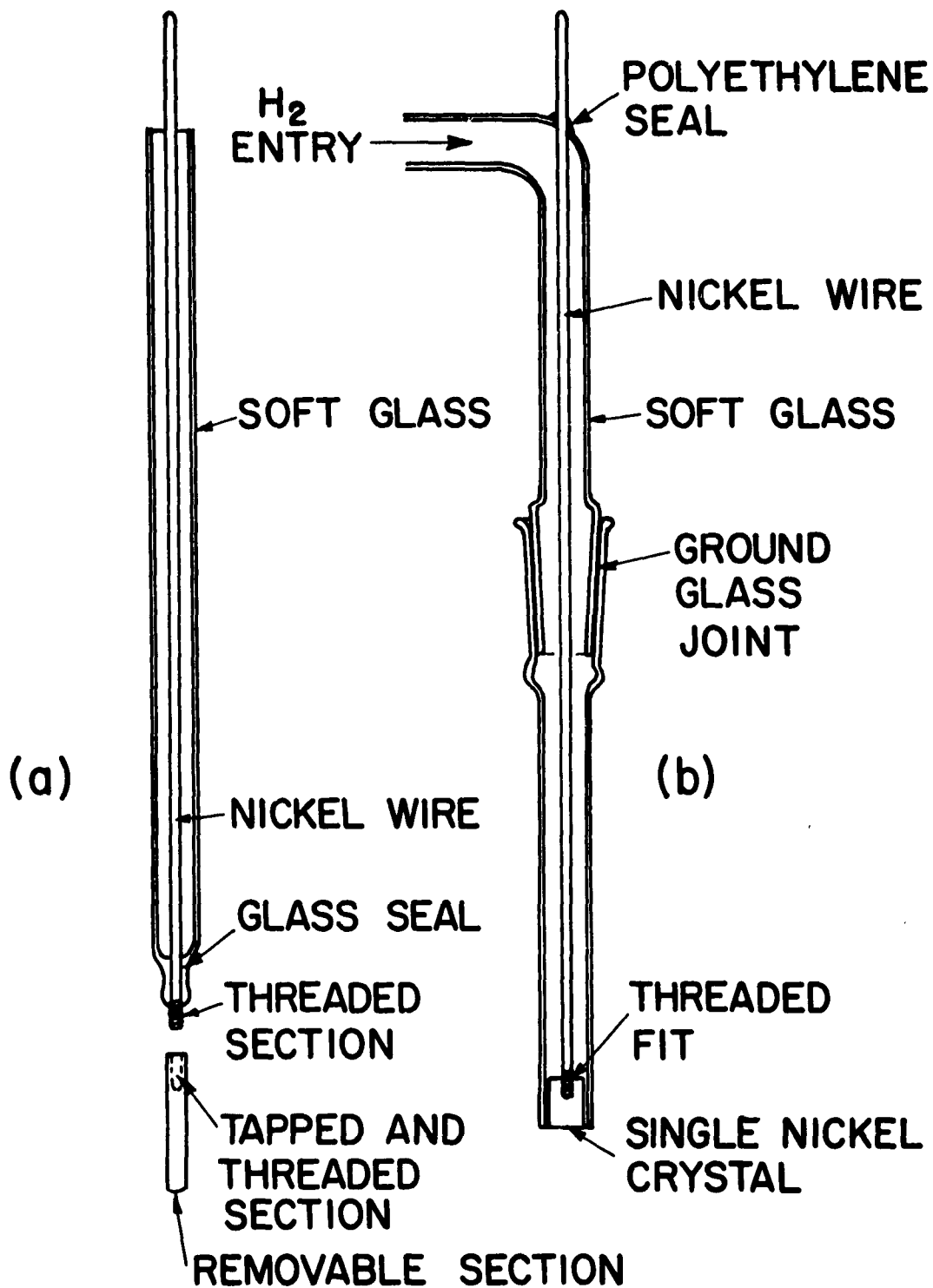


Figure 2. Special electrode designs.

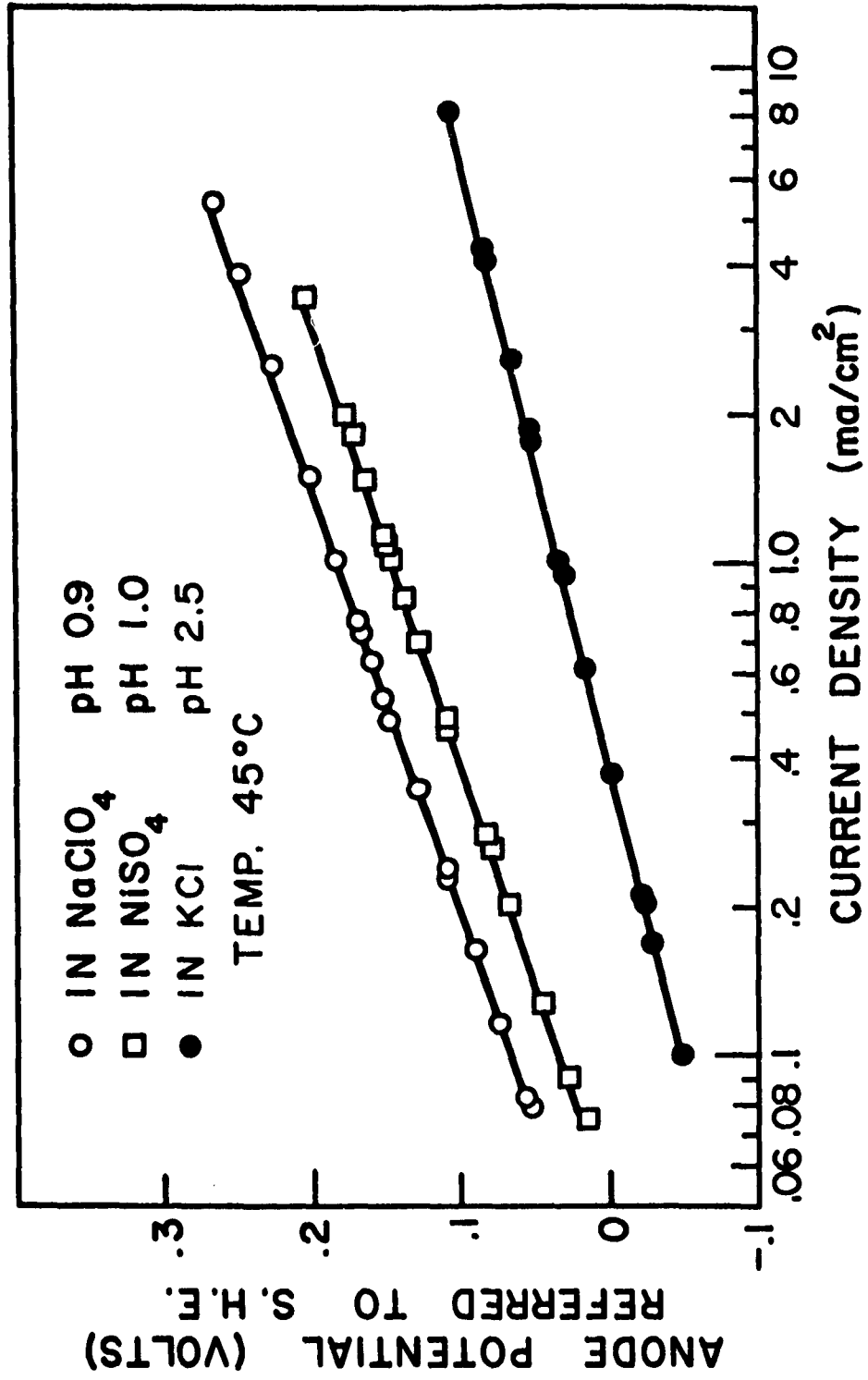


Figure 3. Potential dependence on nature of electrolyte.

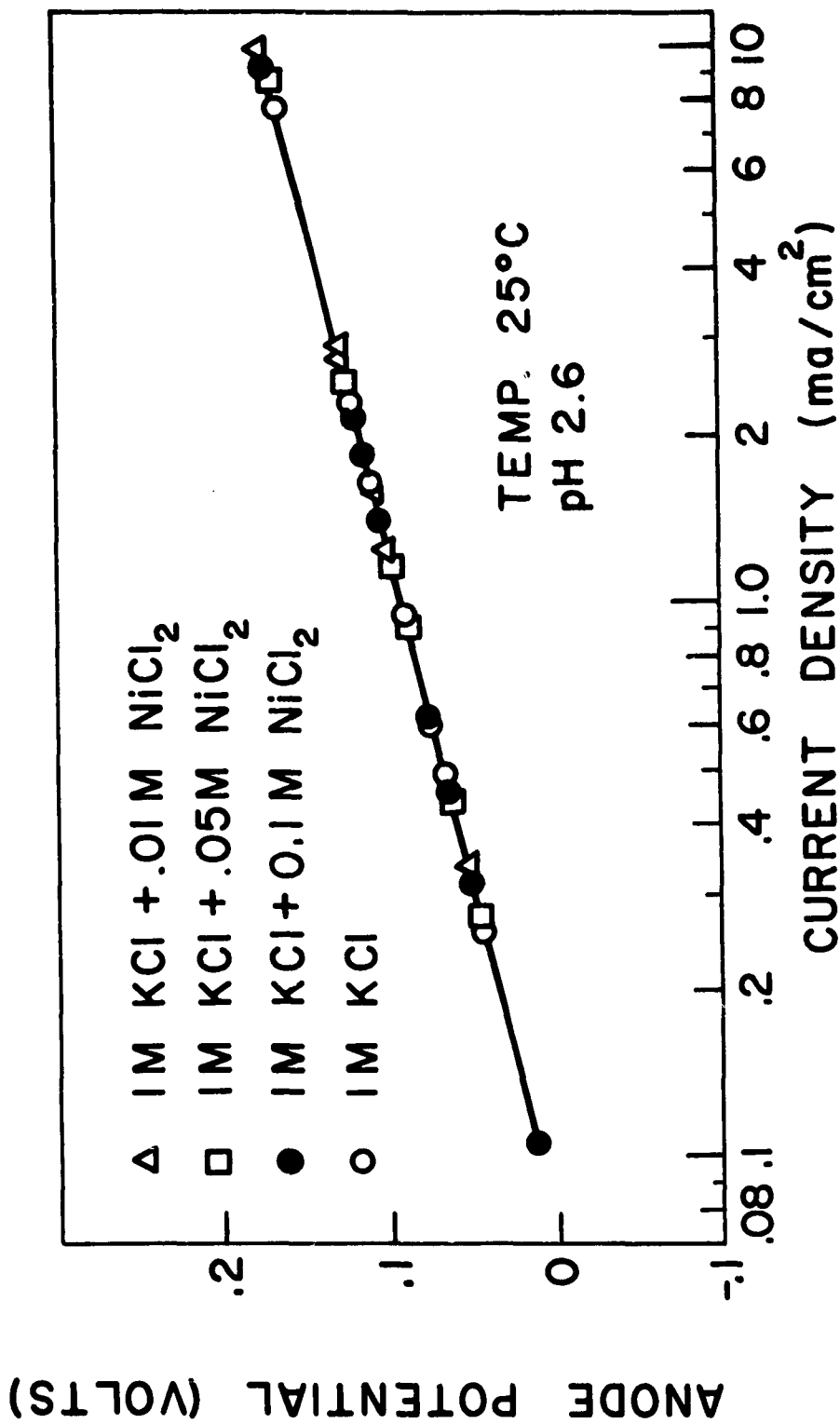


Figure 4. Dependence on addition of NiCl₂ to 1.0 M KCl.

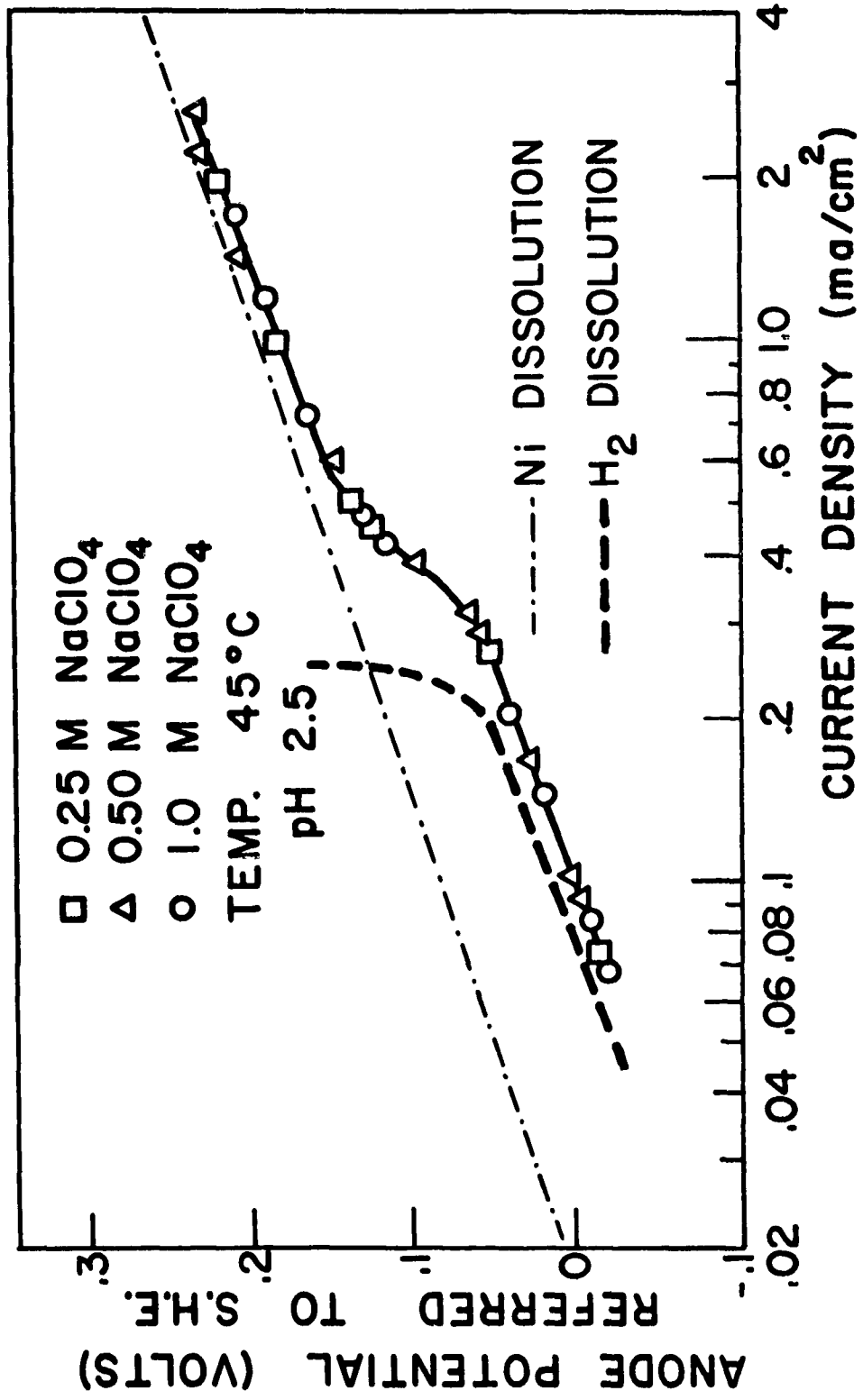


Figure 5. Potential dependence on concentration of NaClO₄.

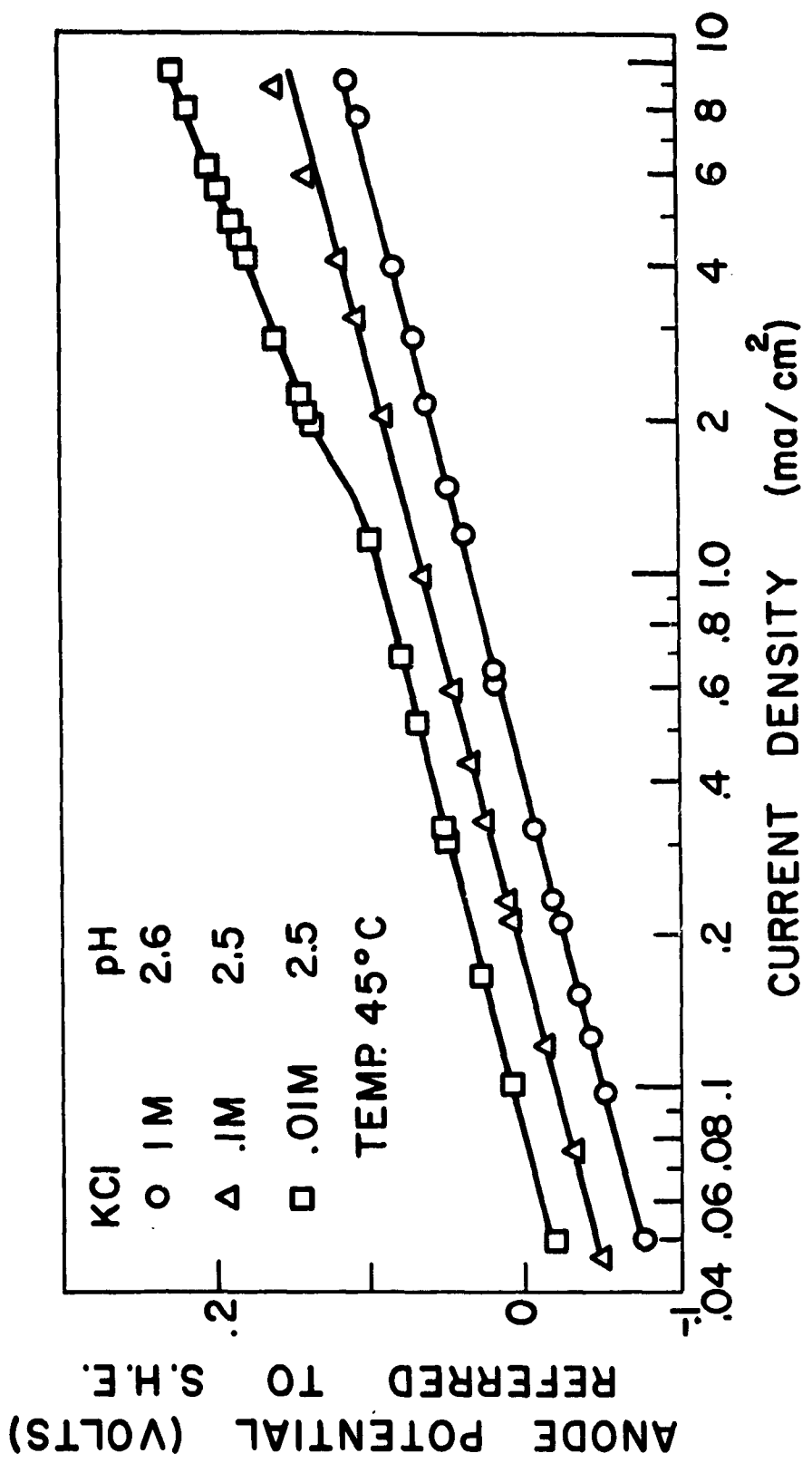


Figure 6. Potential dependence on concentration of KCl.

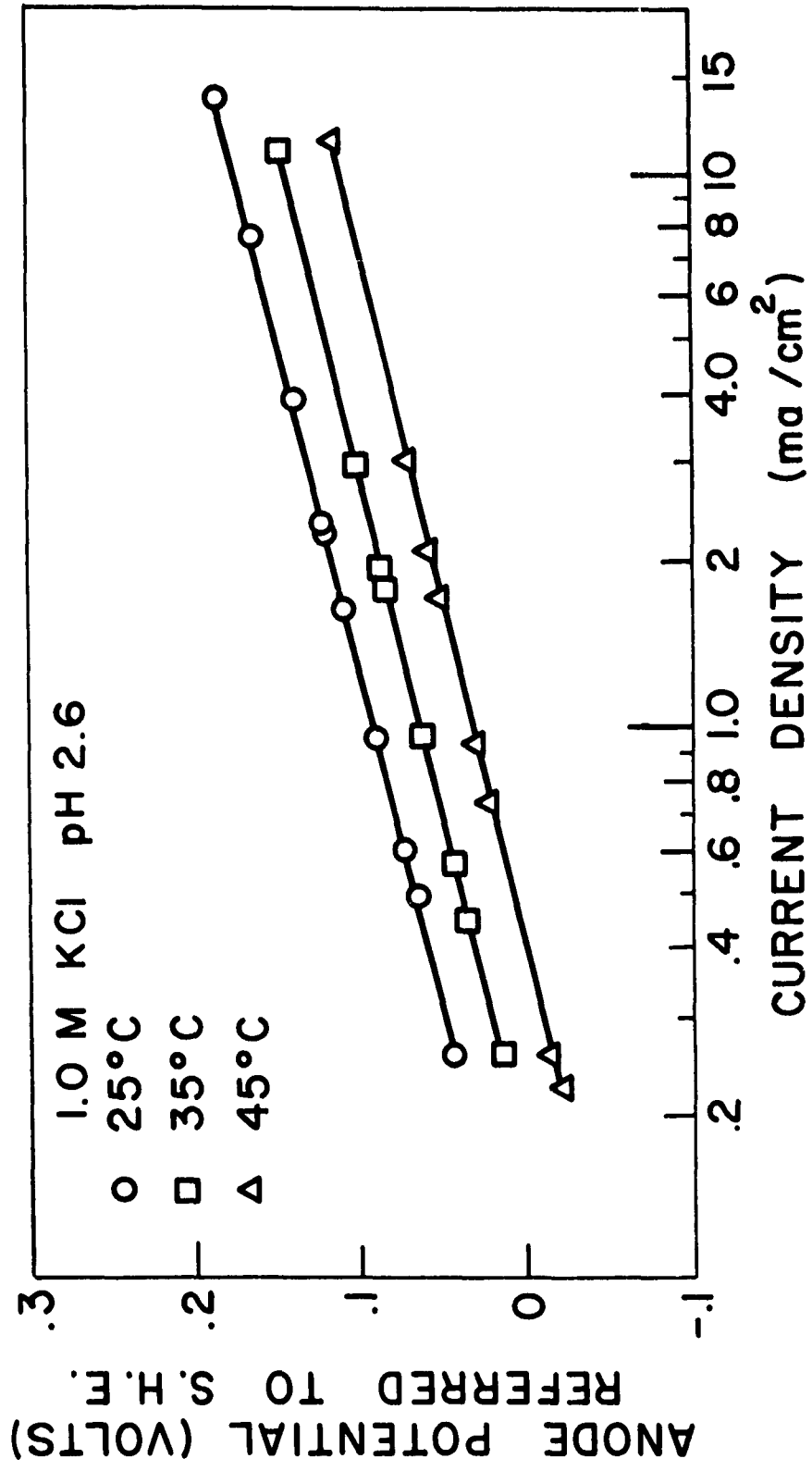


Figure 7. Potential dependence on temperature in 1.0 M KCl.

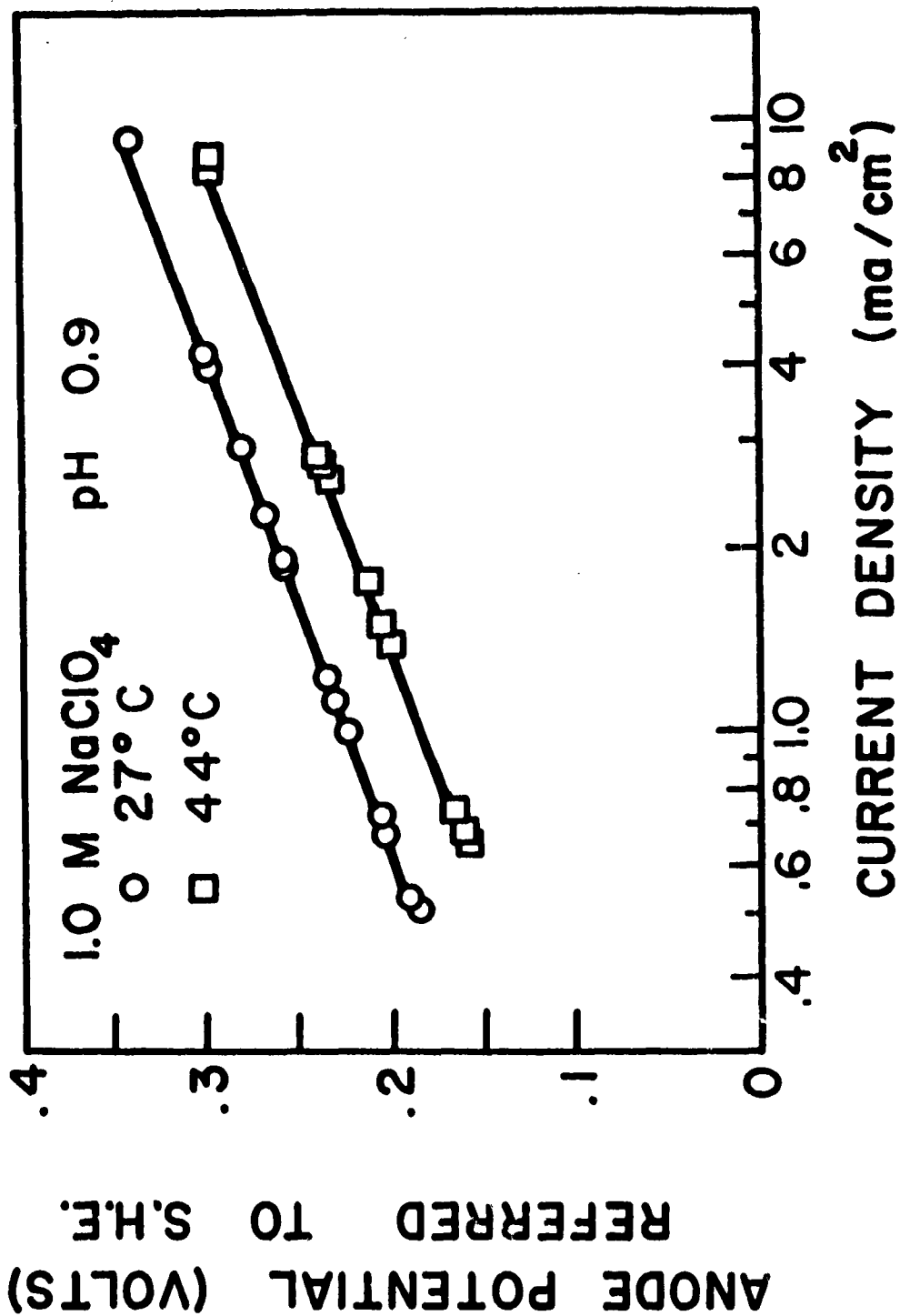


Figure 8. Potential dependence on temperature in 1.0 M NaClO₄.

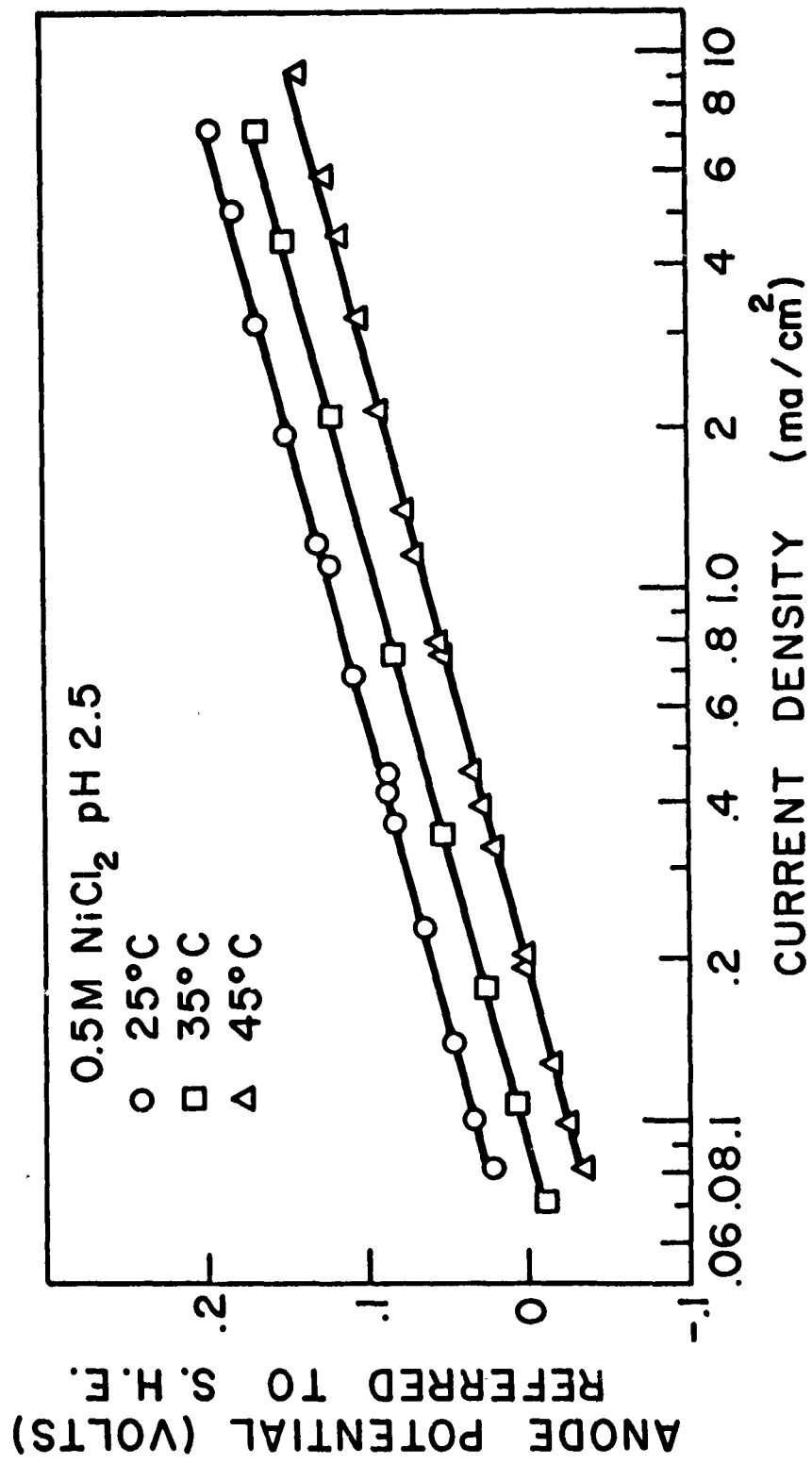


Figure 9. Potential dependence on temperature in 0.5 M NiCl₂.

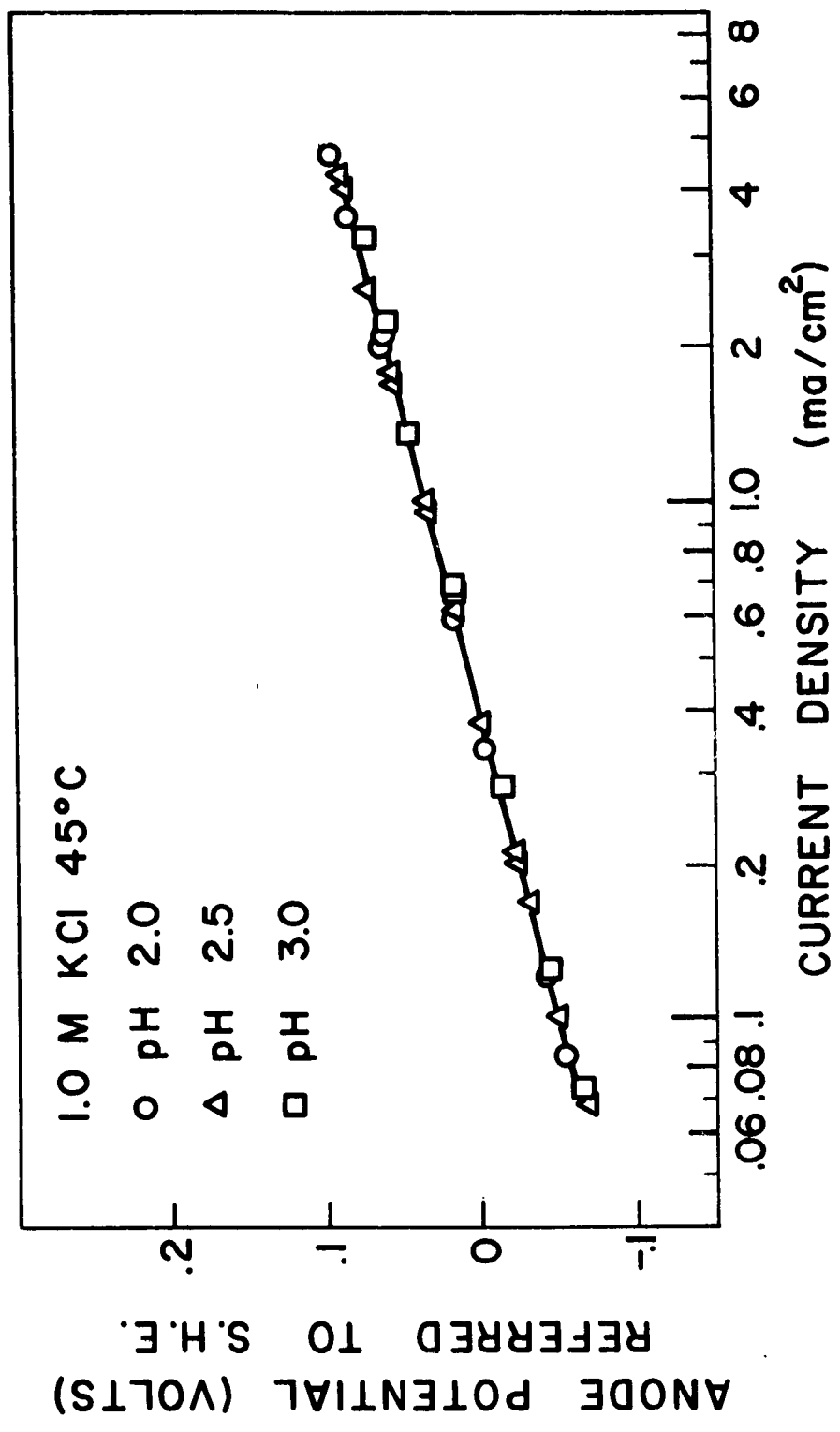


Figure 10. Potential dependence on pH in 1.0 M KCl.

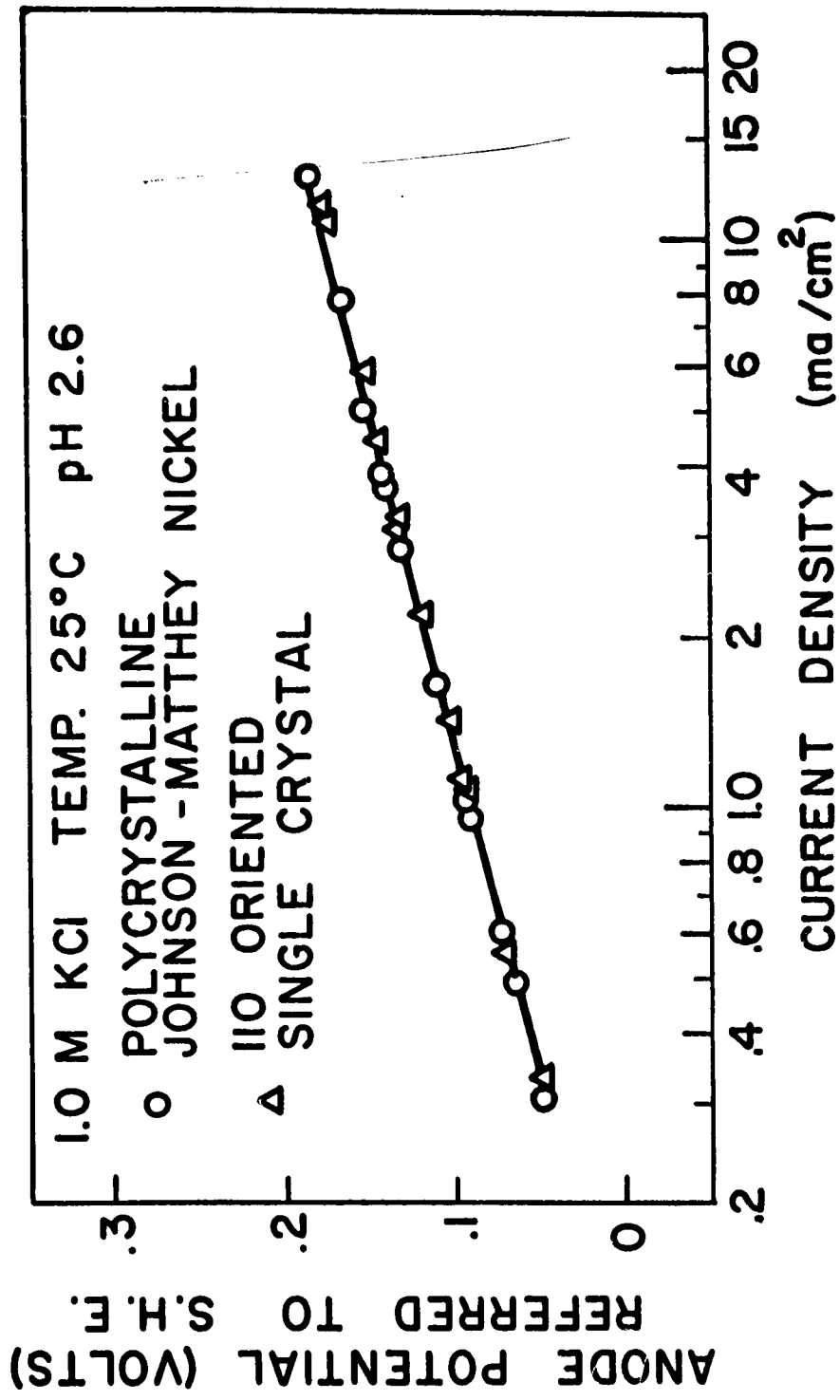


Figure 11. Comparison of polycrystalline and single crystal nickel in 1.0 M KCl.

TECHNICAL REPORT DISTRIBUTION LIST
WESTERN RESERVE UNIVERSITY

Contract 2391(00)

NR No. 359-277

<u>No. Copies</u>	<u>No. Copies</u>
Commanding Officer. Office of Naval Research John Crerar Library Building 86 E. Randolph Street Chicago 1, Illinois (1)	Air Force Office of Scientific Research(SRLT) Washington 25, D. C. (1)
Commanding Officer Office of Naval Research Branch Office 346 Broadway New York 13, New York (1)	Commanding Officer Diamond Ordnance Fuze Laboratories Washington 25, D. C. Attn: Technical Reference Section ORDTL 06.33) (1)
Commanding Officer Office of Naval Research Branch Office 1030 E. Green Street Pasadena 1, California (1)	Office of Chief of Staff (R&D) Department of the Army Pentagon 3B516 Washington 25, D. C. Attn: Chemical Adviser (1)
Commanding Officer Office of Naval Research Branch Office Navy No. 100 Fleet Post Office New York, New York (7)	Chief, Bureau of Ships Department of the Navy Washington 25, D. C. Attn: Code 340 (2)
Director, Naval Research Laborator., Washington 25, D. C. Attn: Technical Information Ctr. (6) Chemistry Division (2)	Chief, Bureau of Naval Weapons Department of the Navy Washington 25, D. C. Attn: Technical Library (3) Code RRMA-3 (1)
Chief of Naval Research Department of the Navy Washington 25, D. C. Attn: Code 425 (2)	ASTIA Document Service Center Arlington Hall Station Arlington 12, Virginia (10)
Technical Library OASD (R&E) Pentagon Room 3E1065 Washington 25, D.C. (1)	Director of Research Signal Corps Eng. Laboratories Fort Monmouth, New Jersey (1)
Technical Director Research & Engineering Division Office of the Quartermaster General Department of the Army Washington 25, D.C. (1)	Naval Radiological Def. Laboratory San Francisco 24, California Attn: Technical Library (1)
Research Director Chemical & Plastics Division Quartermaster Res. & Eng. Command Natick, Massachusetts (1)	Naval Ordnance Test Station China Lake, California Attn: Head, Chemistry Division (1)

Contract 2391(00)
NR No. 359-277

-40-

<u>No. Copies</u>	<u>No. Copies</u>
Commanding Officer Office of Ordnance Research Box CM, Duke Station Durham, North Carolina (1)	Dr. A. Patterson, Jr. Department of Chemistry Yale University New Haven, Connecticut (1)
Brookhaven National Laboratory Chemistry Division Upton, New York (1)	Aerojet General Corporation Azusa, California Attn: Dr. Scott B. Kilmer (1)
Atomic Energy Commission Research Division, Chemistry Branch Washington 25, D. C. (1)	Dr. S. Young Tyree, Jr. Department of Chemistry University of North Carolina Chapel Hill, North Carolina (1)
Atomic Energy Commission Library Branch Technical Information ORE Post Office Box E Oak Ridge, Tennessee (1)	Chief of Naval Operations Department of the Navy Washington 25, D. C. Attn: Op 31 (1) Op 03 (1) Op 09D (1)
U. S. Army Chemical Warfare Labs. Technical Library Army Chemical Center, Maryland (1)	Dr. F. L. Granger, Jr. National Carbon Company P. O. Box 6087 Cleveland 1, Ohio (1)
Office of Technical Services Department of Commerce Washington 25, D. C. (1)	Dr. H. W. Salzberg Department of Chemistry City College New York, New York (1)
National Research Council Committee on Undersea Warfare 2101 Constitution Avenue Washington 25, D. C. (1)	Dr. W. J. Hamer Electrochemistry Section National Science Foundation Washington, D. C. (1)
Commander Submarine Force U. S. Atlantic Fleet Box 27 New London, Connecticut (1)	Dr. T. P. Dirkse Department of Chemistry Calvin College Grand Rapids, Michigan (1)
Commander Submarine Force U. S. Pacific Fleet Fleet Post Office San Francisco, California (1)	Chief, Bureau of Ships Department of the Navy Washington 25, D. C. Attn: Code 660S (1) Code 109 (1) Code 525 (1)
Commander Submarine Develop. Group Box 70 New London, Connecticut (1)	
Dr. Paul Delahay Department of Chemistry Louisiana State University Baton Rouge, Louisiana (1)	

Contract 2391(00)
NR No. 359-277

-41-

	<u>No. Copies</u>		<u>No. Copies</u>
ONR Resident Representative University of Michigan 820 E. Washington Street Ann Arbor, Michigan	(1)	Mr. B. R. Stein European Research Office U. S. Army R & D. Liaison APO 757 New York, New York	(1)
Dr. George J. Janz Department of Chemistry Rensselaer Polytechnic Institute Troy, New York	(1)	Dr. E. M. Cohn Army Research Office Office of Chief of R&D Department of the Army The Pentagon Washington 25, D. C.	(1)
Dr. Morris Eisenberg Missile Systems Division Lockheed Aircraft Corporation Sunnyvale, California	(1)	Mr. E. R. Rechel Building 110 Frankford Arsenal Bridge and Tacony Streets Philadelphia 37, Pennsylvania	(1)
Dr. G. Barth-Wehrenalp Pennsalt Chemical Corporation P. O. Box 4388 Philadelphia 18, Pennsylvania	(2)	Monsanto Chemical Company Research and Engineering Division Boston 49, Massachusetts Attn: Mr. K. Warren Easley	(1)
Dr. B. R. Sundheim Department of Chemistry New York University New York 3, New York	(1)	Lawrence R. Anderson Lt. Colonel, GS Acting Chief Physical Sciences Division Department of the Army Army Research Office Washington 25, D. C.	(1)
Dr. R. A. Marcus Department of Chemistry Polytechnic Institute of Brooklyn Brooklyn 1, New York	(1)	E. C. Wadlow Department of Material Research Queen Anne Mansions St. James Park London, S.W. 1, England	(1)
Commanding Officer U. S. Naval Underwater Ordnance Station Newport, Rhode Island	(1)	Via: Commanding Officer Office of Naval Research Branch Office, Navy No. 100 Fleet Post Office New York, New York	
Commanding Officer U. S. Naval Ordnance Laboratory Corona, California Attn: Library	(1)	Dr. G. M. Cohn NASA Code RPP 1512 H Street, N. W. Washington 25, D. C.	(1)
Dr. G. J. Young Department of Ceramics Alfred University Alfred, New York	(1)		
Dr. M. S. Cohen Propellants Synthesis Section Reaction Motors Division Danville, New Jersey	(1)		

Contract 2391(00)
NR No. 359-277

No. Copies

Sandia Corporation
Sandia Base
Albuquerque, New Mexico (1)

Dr. G. C. Szego
Institute for Defense Analysis
1666 Connecticut Ave., N. W.
Washington 9, D. C. (1)

Material Lab. Library Bldg. 291
Code 912B
New York Naval Shipyard
Brooklyn 1, New York (1)

Dr. Leonard Nanis
School of Mines
Columbia University
New York 27, New York (1)